Author(s): Zaulet, Adnana; Nuez, Miquel; Sillanpää, Reijo; Teixidor, Francesc; Viñas, Clara

Title: Towards purely inorganic clusters in medicine : biocompatible divalent cations as counterions of cobaltabis(dicarbollide) and its iodinated derivatives

Year: 2021

Version: Published version

Please cite the original version:

Zaulet, A., Nuez, M., Sillanpää, R., Teixidor, F., & Viñas, C. (2021). Towards purely inorganic clusters in medicine : biocompatible divalent cations as counterions of cobaltabis(dicarbollide) and its iodinated derivatives. Journal of Organometallic Chemistry, 950, Article 121997. https://doi.org/10.1016/j.jorganchem.2021.121997

Journal of Organometallic Chemistry 950 (2021) 121997

Contents lists available at ScienceDirect

Journal of Organometallic Chemistry

journal homepage: www.elsevier.com/locate/jorganchem

Towards purely inorganic clusters in medicine: Biocompatible divalent cations as counterions of cobaltabis(dicarbollide) and its iodinated derivatives ☆

Adnana Zaulet [a], Miquel Nuez [a], Reijo Sillanpää [b], Francesc Teixidor [a], Clara Viñas [a,*]

[a] Institut de Ciència de Materials de Barcelona, ICMAB-CSIC, Campus Universitat Autònoma de Barcelona, 08193 Bellaterra, Spain
[b] Dept. of Chemistry, University of Jyväskylä, FIN-40014, Jyvaskyla, Finland

ARTICLE INFO

Article history:
Received 30 April 2021
Revised 12 July 2021
Accepted 17 July 2021
Available online 22 July 2021

Keywords:
Metallacarboranes
Iodine
Calcium
Dual-action
Biocompatible
X-ray contrast
Bone biomaterials

ABSTRACT

Monovalent cations, Cs^+, and alkylammonium ($[NR_4]^+$) salts have traditionally been used to precipitate the anions of boranes, carborane and metallocarborane clusters. In contrast, in the body and in living organisms in general, divalent cations have a special relevance. In this work, we isolate for the first time the cobaltabis(dicarbollide) salts of the biocompatible divalent cations of biological importance that can have application both in biology and in materials science. The preparation of Ca^{2+}, Mg^{2+} and Fe^{2+} salts of anionic iodinated *nido*-$[C_2B_9H_{12}]^-$ and cobaltabis(dicarbollide) as well as its di-, tetra- and octa-iodinated derivatives are reported. Ca^{2+} and Mg^{2+} are hard Lewis acids and thus forms aqua ions if water is present in the synthetic process. All solid Ca^{2+} and Mg^{2+} salts studied in this work contained water molecules coordinated that have been detected by IR and TGA/DSC. Fe^{2+} is a medium hard Lewis acid and Fe^{3+} is a hard one. In acetone they do not coordinate to cobaltabis(dicarbollide) anion, but are solvated by acetone. The studied Ca^{2+} salts of iodinated cobaltabis(dicarbollide) are basically inorganic small molecules that provide at once the biocompatible divalent Ca^{2+} cation and and iodinated anions thus simultaneously providing an X-ray contrast agent and/or bone defect repairing agent in regenerative medicine.

1. Introduction

A long list of inorganic elements, many of them ionic, play essential biological roles for life. The proper functioning of the human body depends, among other factors, on the so-called divalent cations, which have chemical peculiarities that make them extremely important for our body [1]. The divalent cations Mg (e.g. binding to ATP and other nucleotides), Ca (e.g. calmodulin and hydroxylapatite in bones), and Fe (in red blood cells e.g. Hemoglobin, Cytochromes and in muscle cells called myoglobin) are, among others such Mn, Cu, Zn, Mo, essential elements in humans and, [2] furthermore, Co is a necessary component of vitamin B12 [3].

Bone is one of the most impressive natural composite material made of mineral and organic matrices that provide stiffness (for support and leverage) and toughness (for protection and impact resistance) [4]. The chemical composition of the bone mineral matrix is in the form of nanosized carbonated calcium phosphate particles. These particles are preferably elongated aligned along the long axis of type I collagen fibrils, which are components of the organic matrix [5]. Furthermore, the Ca^{2+} cations have been shown to act as an adhesive by exhibiting great versatility in interacting with proteins to form biomaterials that are more complex [6].

Osteoporosis, which is usually related with aging demineralization and weakening of bone, produces fractures at the vertebra by compression. An estimated number of 1.4 million new osteoporotic vertebral fractures occurs worldwide every year in patients over 50 years of age [7]. The patients' treatment with one or more vertebral compression fractures is nowadays done by using the vertebroplasty technique [8]. Vertebroplasty comprises percutaneous injection of cement into a weakened osteoporotic vertebral element. The cement provides additional strength and stiffness after hardening in situ, causing effective pain reduction, both in the short term and in the long term resulting in a significant improvement of quality of life in the elderly population [7]. Bone cements for vertebroplasty require a higher level of radiocontrast than cements for knee or hip arthroplasty [9]. This is generally accomplished by adding a relatively large portion of $BaSO_4$, although this affects the

☆ Dedicated to Prof. Elena Shubina in recognition to her scientific contribution to non-covalent interactions in Organometallic Chemistry on the occasion of her 70th birthday.

* Corresponding author.
E-mail address: clara@icmab.es (C. Viñas).

https://doi.org/10.1016/j.jorganchem.2021.121997

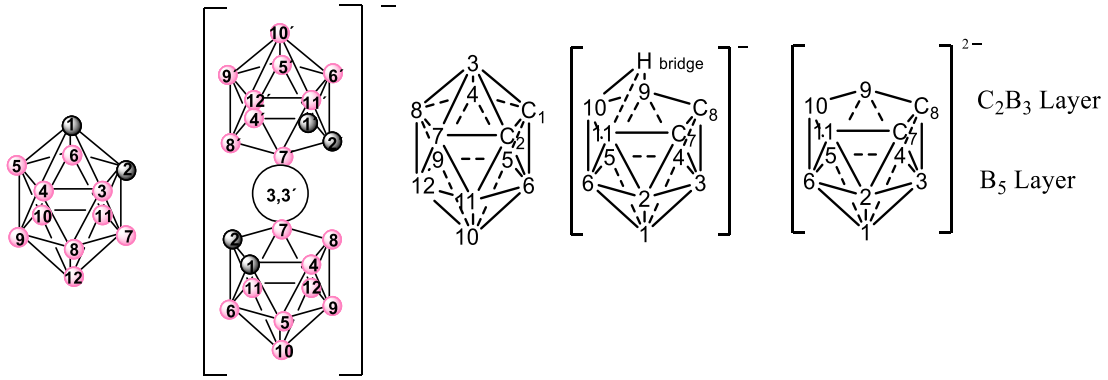

Chart 1. Icosahedral 1,2-*closo*-$C_2B_{10}H_{12}$, [7,8-*nido*-$C_2B_9H_{12}$]$^-$ and [3,3'-Co(1,2-$C_2B_9H_{11}$)$_2$]$^-$ with their vertexes numbering.

physical-mechanical and biological properties of the cement. This prompted to develop an alternative radiopaque cement, on the basis of highly radiopaque methacrylic biomaterials. In this regard, highly iodinated molecules have been of interest in materials science and medical applications as next generation of radiopaque contrast agents for X-ray diagnosing imaging [10].

The stability of the 3D rigid and aromatic framework of neutral icosahedral $C_2B_{10}H_{12}$ carboranes and anionic carboranes and cobaltabis(dicarbollides), [$CB_{10}H_{11}$]$^-$ and [Co($C_2B_9H_{11}$)$_2$]$^-$, [11] might be merged with the capacity to functionalize the different vertexes with different ending branches to provide multimodal treatments, i.e. diagnosis + therapy in addition to perform as drug delivery nanocarriers. This is why the role of carboranes and metallabis(dicarbollides) in medicinal chemistry has diversified in recent years [12] and now extends into areas of biosensors, biomimetic materials, drug discovery, molecular imaging, and targeted radionuclide therapy [13].

About it and earlier in our group, [14] the stable tetraiodocarborane 8,9,10,12-I_4-*closo*-$C_2B_{10}H_8$ with high iodine content (78.4%) was tested as X-ray contrast agent in acrylic methylmetacrylate bone cements due to its, exceptional stability, total insolubility in aqueous media, good cell viability, good contact biocompatibility as well as a satisfactory radiopacity [14].

The partial deboronation reaction of the *closo*-1,2-$C_2B_{10}H_{12}$ cluster leads to the corresponding anionic [7,8-*nido*-$C_2B_9H_{12}$]$^-$ species [15–18]. Following deprotonation, the dianionic [7,8-*nido*-$C_2B_9H_{11}$]$^{2-}$ ligands, that may be interpreted as having an η^5 pentagonal C_2B_3 open face can undergo metal complexation to yield the $\boldsymbol{\theta}$ shape anionic metallabis(dicarbollide) clusters. The most studied of them are the metallabis(dicarbollide), [3,3'-M(1,2-$C_2B_9H_{11}$)$_2$]$^-$, M= Co, Fe, Ni, [19] (Chart 1). If the starting *closo* icosahedral carborane cluster is iodinated or highly iodinated at the boron vertices, the corresponding anionic species either *nido*- or metallabis(dicarbollide) would have iodine atoms bonded to the boron vertices of the respective clusters (Scheme 1).

Previously, [20] we reported the biocompatible alkaline salts (Li, Na and K) of cobaltabis(dicarbollide) but, the biocompatible divalent cations (Fe, Mg and Ca), which are very important for the application of anionic clusters in nanomedicine, [12] remain unknown. Following our studies, in this work, we report the syntheses of the iron, calcium and magnesium salts of the [3,3'-Co(1,2-$C_2B_9H_{11}$)$_2$]$^-$ anion as well as the calcium salts of anionic iodinated *nido*- and *closo* cobaltabis(dicarbollide) clusters. The calcium salts of the iodinated anionic clusters are purely inorganic small molecules that incorporating the biocompatible Ca and iodine atoms at once may offer an opportunity to be applied as X-ray contrast in regenerative medicine and/or in bone defect repair.

2. Results and discussions

2.1. Preparation of the Iron(II) and Iron(III) salts of [3,3'-Co(1,2-$C_2B_9H_{11}$)$_2$]$^-$

Silver salt of cobaltabis(dicarbollide), Ag[3,3'-M(1,2-$C_2B_9H_{11}$)$_2$], [21] was used as precursor to prepare the corresponding Fe^{2+} and Fe^{3+} salts. These iron(II) and iron(III) salts of cobaltabis(dicarbollide) were obtained under a nitrogen atmosphere by adding either $FeCl_2$ or $FeCl_3$ to a concentrated deoxygenated ethanol solution of the silver salt in the stoichiometric ratio 1/2 or 1/3 for Fe^{2+} and Fe^{3+}, respectively, as shown in Scheme 2. The white precipitate that forms (AgCl) was discarded and the orange/brownish solutions concentrated. All the compounds were characterized by ^{1}H, ^{1}H{^{11}B}, ^{11}B, ^{11}B {^{1}H} and ^{13}C{^{1}H}-NMR and FTIR spectroscopy as well as MALDI-TOF-MS.

The IR spectrum of both salts presents a sharp band at around 2564-2517 cm^{-1} typical of the B-H vibration and characteristic bands at 3529 and 1607 cm^{-1} and 3508 and 1609 cm^{-1} for Fe^{2+} and Fe^{3+} salts, respectively, which correspond to the presence of coordinated H_2O. The endothermic weight loss around 140°C at the Thermogravimetric analysis and Differential Scanning Calorimetry (TGA/DSC) for the Fe[3,3'-Co(1,2-$C_2B_9H_{11}$)$_2$]$_3$ is consistent with the existence of coordinated H_2O.

A comparison between the coupled ^{1}H-NMR spectrum (red) and the decoupled ^{1}H{^{11}B}-NMR (blue) of Fe[3,3'-Co(1,2-$C_2B_9H_{11}$)$_2$]$_3$ and Fe[3,3'-Co(1,2-$C_2B_9H_{11}$)$_2$]$_2$ is illustrated in Fig. 1a and 1b; the signal that appears at the lowest field belongs to the H bonded to the carbon cluster atoms. By overlapping the ^{1}H{^{11}B}-NMR spectra of Fe[3,3'-Co(1,2-$C_2B_9H_{11}$)$_2$]$_3$ and Fe[3,3'-Co(1,2-$C_2B_9H_{11}$)$_2$]$_2$ compounds, it is observed that the proton resonances of the paramagnetic Fe^{3+} salt are shifted downfield compared to the chemical shift of the signals for the diamagnetic Fe^{2+} (Fig. 1c). The most affected proton atoms of Fe[3,3'-Co(1,2-$C_2B_9H_{11}$)$_2$]$_3$ are these bonded to B(9,12) and B(8), but the differences are not large suggesting stronger second coordination sphere interactions in Fe^{3+} species.

The ^{11}B{^{1}H}-NMR spectra of Fe[3,3'-Co(1,2-$C_2B_9H_{11}$)$_2$]$_3$ and Fe[3,3'-Co(1,2-$C_2B_9H_{11}$)$_2$]$_2$ species display a similar pattern but the full spectrum of the Fe^{3+} is also shifted upfield with respect to the Fe^{2+} (Fig. 2). The influence of the paramagnetic Fe^{3+}, which acts as countercation in Fe[3,3'-Co(1,2-$C_2B_9H_{11}$)$_2$]$_3$, produces a noticeable but small effect on the ^{11}B{^{1}H}-NMR spectrum of the anionic [3,3'-Co(1,2-$C_2B_9H_{11}$)$_2$]$^-$ cluster (^{11}B{^{1}H} NMR spectrum range is from +9 to -22 ppm). While, the paramagnetic Fe^{3+} produces a very large effect in the ^{11}B{^{1}H}-NMR spectrum of the anionic [3,3'-Fe(1,2-$C_2B_9H_{11}$)]$^-$ cluster in which Fe^{3+} is part of the cluster (^{11}B{^{1}H} NMR spectrum range is from +30 to -550 ppm) [22].

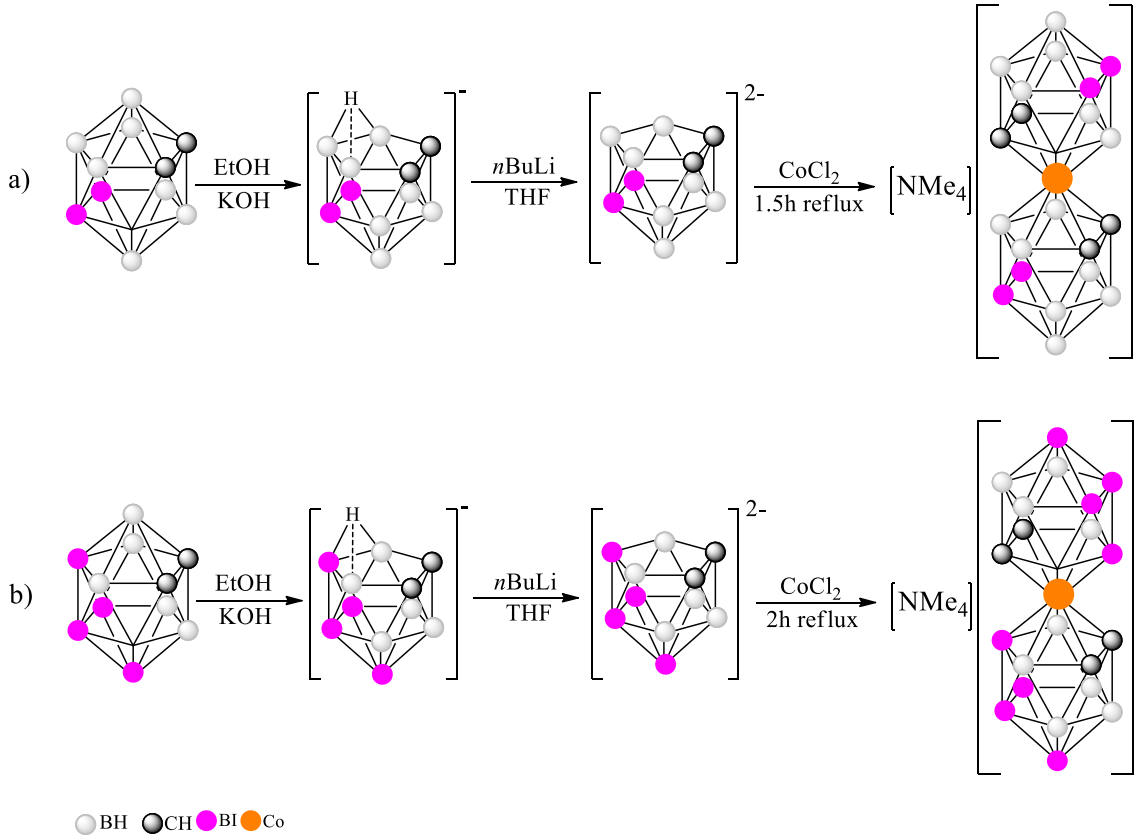

Scheme 1. Procedures for the synthesis of tetra- and octa-iodinated at the boron vertices of cobaltabis(dicarbollide) derivatives, respectively. Circles in dark grey represent the C_c-H vertices while the ones in light and dark pink correspond to B-H and B-I vertices and the orange and circles to Co. [24].

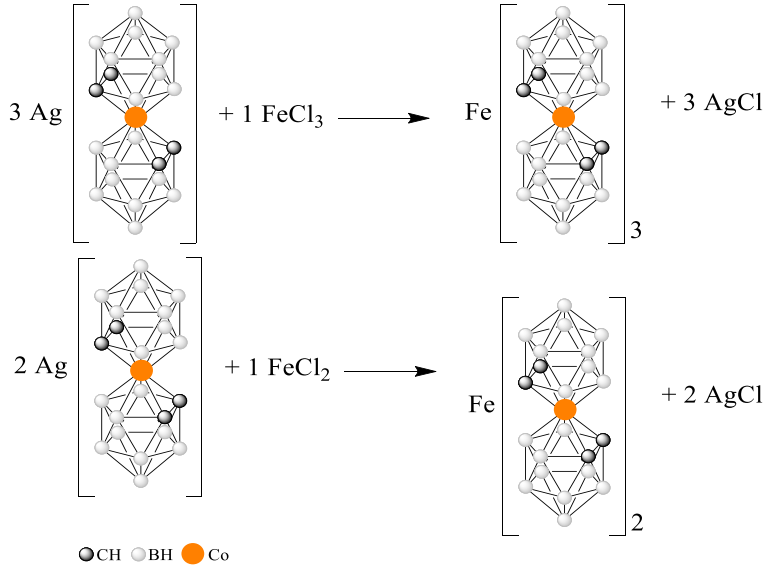

Scheme 2. Synthesis of the iron salts of cobaltabis(dicarbolloide), $Fe[3,3'\text{-}Co(1,2\text{-}C_2B_9H_{11})_2]_2$ and $Fe[3,3'\text{-}Co(1,2\text{-}C_2B_9H_{11})_2]_3$.

2.2. Preparation of the calcium and magnesium salts of $[3,3'\text{-}Co(1,2\text{-}C_2B_9H_{11})_2]^-$ and $[3,3'\text{-}Co(8\text{-}I\text{-}1,2\text{-}C_2B_9H_{10})_2]^-$

The calcium and magnesium salts of $[3,3'\text{-}Co(1,2\text{-}C_2B_9H_{11})_2]^-$ and $[3,3'\text{-}Co(8\text{-}I\text{-}1,2\text{-}C_2B_9H_{10})_2]^-$ were obtained from $[NMe_4][3,3'\text{-}Co(1,2\text{-}C_2B_9H_{11})_2]$ and $Cs[3,3'\text{-}Co(8\text{-}I\text{-}1,2\text{-}C_2B_9H_{10})_2]$ by using cationic exchange resin loaded with Ca^{2+} or Mg^{2+} cations, respectively (Fig. 3). After the preparation, the compounds were characterized employing spectroscopic techniques such as ATR, MALDI-TOF-MS, ^{1}H- and ^{11}B-NMR. A unique peak at m/z corresponding to the anion peak with a separation of one unit between isotopic peaks distribution was observed at the MALDI-TOF-MS spectra for all four salts. The $[NMe_4]^+$ cationic exchange by Ca^{2+} and Mg^{2+} in the salts of $[3,3'\text{-}Co(1,2\text{-}C_2B_9H_{11})_2]^-$ was confirmed by comparing their IR and NMR spectra while, in the case of the $Cs[3,3'\text{-}Co(8\text{-}I\text{-}1,2\text{-}C_2B_9H_{10})_2]$ was confirmed by the presence

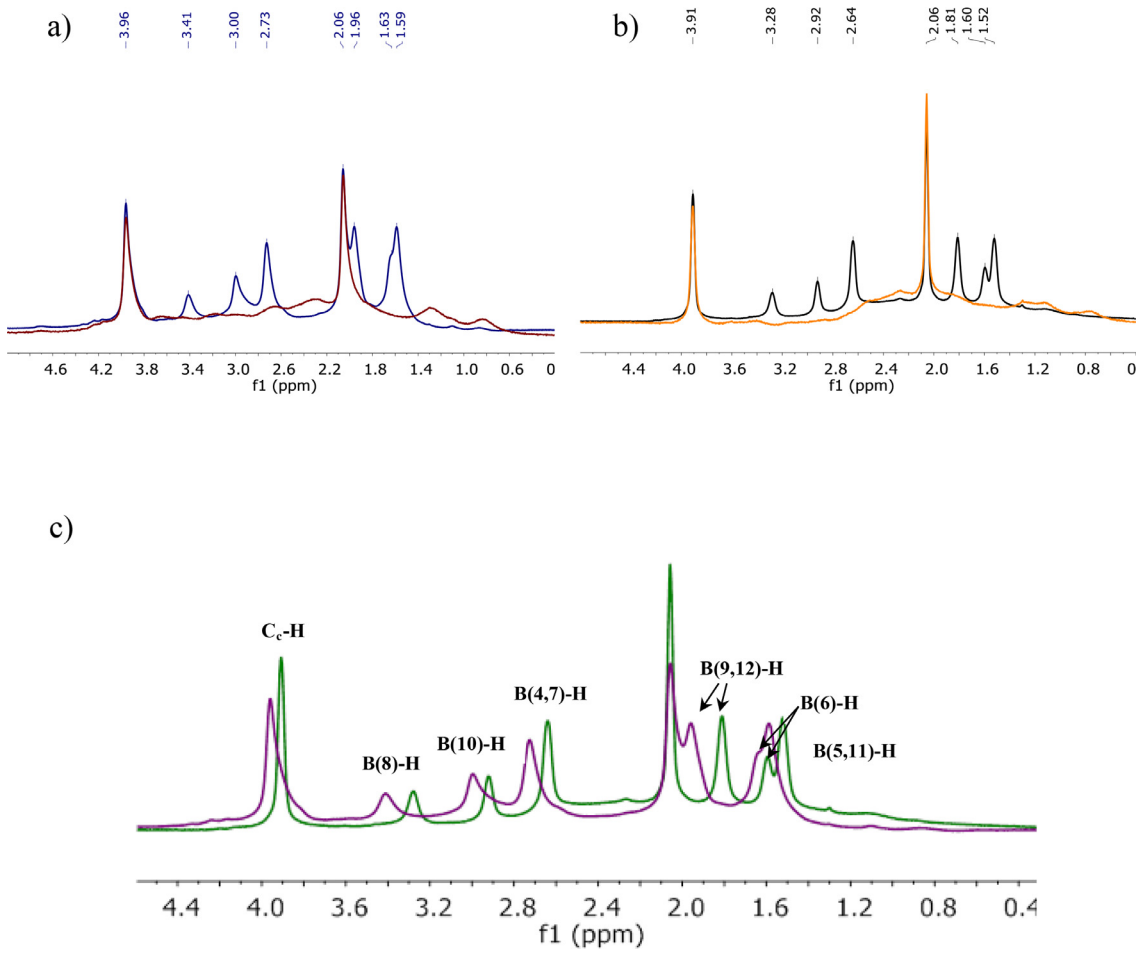

Fig. 1. a) Comparison between ^{1}H-NMR (red) and ^{1}H{^{11}B}-NMR (blue) for salt Fe[3,3'-Co(1,2-$C_2B_9H_{11}$)$_2$]$_3$. b) Comparison between ^{1}H-NMR (orange) and ^{1}H{^{11}B}-NMR (black) for compound Fe[3,3'-Co(1,2-$C_2B_9H_{11}$)$_2$]$_2$. c) ^{1}H{^{11}B}-NMR comparison between Fe[3,3'-Co(1,2-$C_2B_9H_{11}$)$_2$]$_2$ (green) and Fe[3,3'-Co(1,2-$C_2B_9H_{11}$)$_2$]$_3$ (purple).

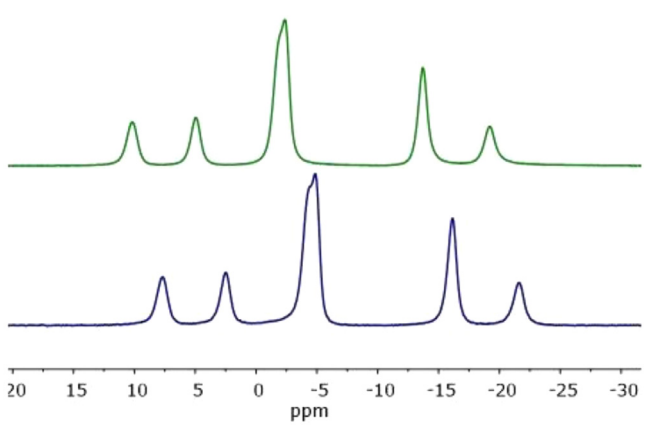

Fig. 2. Comparison of ^{11}B-NMR spectra of the Fe[3,3'-Co(1,2-$C_2B_9H_{11}$)$_2$]$_2$.(green) and Fe[3,3'-Co(1,2-$C_2B_9H_{11}$)$_2$]$_3$ (blue).

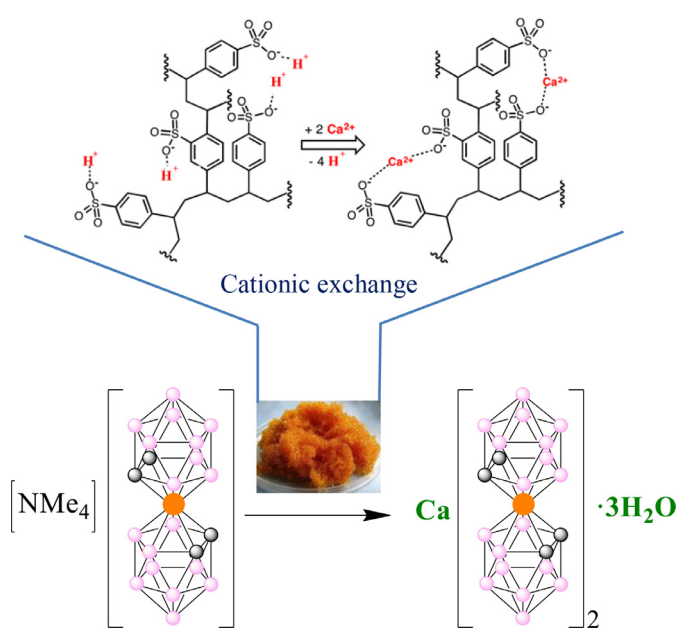

Fig. 3. Preparation of Ca[3,3'-Co(1,2-$C_2B_9H_{11}$)$_2$]·3H_2O.

of coordinated water in the IR and TGA/DSC. Cs(I) is a weak Lewis acid with low hydration energy and thus it does not form $[Cs(H_2O)_n]^+$ ions within these salts while, Ca^{2+} and Mg^{2+} are hard Lewis acids and thus form aqua ions if water is present in the synthetic process with most of the anions. The IR spectra of both Ca^{2+} and Mg^{2+} salts display strong bands in the ranges 3540/3516 and 1644/1602 cm^{-1} that are assigned in that order to the ν(O-H) and δ(H-O-H) of the coordinated H_2O but, highlighting that the related strongest bands correspond to Mg^{2+} salts because Mg^{2+} is stronger Lewis acid than Ca^{2+}. This agrees with the Irving-Williams stability series that postulates the stability of alkaline earth metal ion complexes for a given ligand, in our case would be

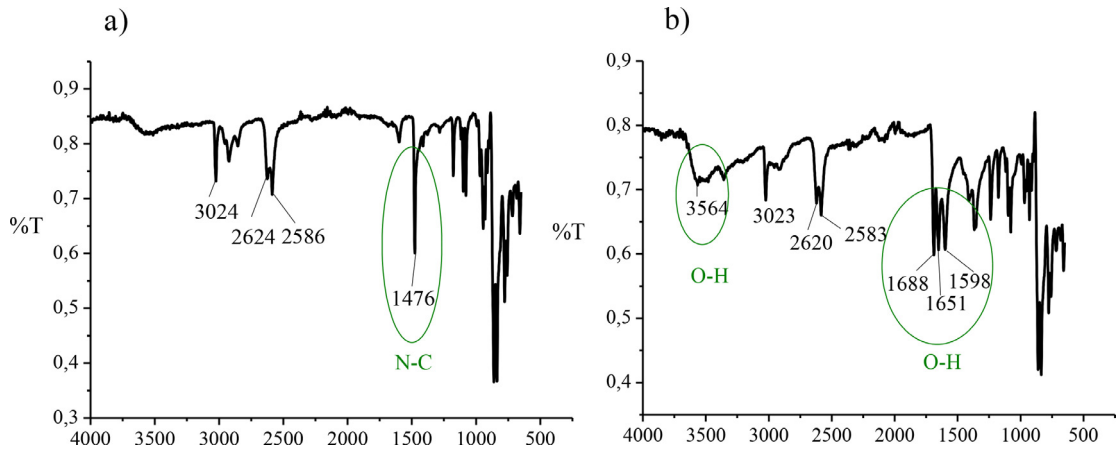

Fig. 4. IR spectra of a) $[NMe_4][3,3'\text{-}Co(8,9,10,12\text{-}I_4\text{-}1,2\text{-}C_2B_9H_7)_2]$ and b) $Ca[3,3'\text{-}Co(8,9,10,12\text{-}I_4\text{-}1,2\text{-}C_2B_9H_7)_2]_2{\cdot}5H_2O$.

$[3,3'\text{-}Co(1,2\text{-}C_2B_9H_{11})_2]^-$ and $[3,3'\text{-}Co(8\text{-}I\text{-}1,2\text{-}C_2B_9H_{10})_2]^-$, increase in the order $Ba^{2+} < Sr^{2+} < Ca^{2+} < Mg^{2+}$ [23]. The stretching $\nu(C_{cluster}\text{-}H)$ and ν(B-H) bands corresponding to the cluster's vertices in these salts appear in the ranges 3039/3040 and 2584/2512 cm^{-1}, respectively.

To learn on the coordinated water molecules to the Ca^{2+}, Thermogravimetric analysis/Differential Scanning Calorimetry (TGA/DSC) was run. In the all salts, an endothermic weight process is observed until 120°C. In the case of $Ca[3,3'\text{-}Co(8\text{-}I\text{-}1,2\text{-}C_2B_9H_{10})_2]$ two endothermic processes at 105 and 160°C with weight loses of 4.17 and 8.98%, respectively relates the loss of coordinated H_2O and an iodine atom. TGA plus elemental analysis of the calcium salts of the $[3,3'\text{-}Co(1,2\text{-}C_2B_9H_{11})_2]^-$ and $[3,3'\text{-}Co(8\text{-}I\text{-}1,2\text{-}C_2B_9H_{10})_2]^-$ anions indicates that the coordination number of H_2O is 3 in both salts.

2.3. Isolation of the calcium salts of highly iodinated cobaltabis(dicarbollide) derivatives

Knowing that the chemical composition of the bones is around 45% minerals (calcium carbonates and phosphates), we had in mind the use of such highly iodinated anionic compounds with Ca^{2+} as a bone component which would enable the application of these salts as X-ray contrast in vertebroplasty.

Thus, the iodinated at the boron vertices of the anionic *nido*-carboranes, $[HNMe_3][5,6\text{-}I_2\text{-}7,8\text{-}nido\text{-}C_2B_9H_{10}]$, $[HNMe_3][1,5,6,10\text{-}I_4\text{-}7,8\text{-}nido\text{-}C_2B_9H_8]$, and cobaltabis(dicarbollide) species, $[NMe_4][3,3'\text{-}Co(9,12\text{-}I_2\text{-}1,2\text{-}C_2B_9H_9)_2]$ and $[NMe_4][3,3'\text{-}Co(8,9,10,12\text{-}I_4\text{-}1,2\text{-}C_2B_9H_7)_2]$ were obtain by indirect route as previously reported (Scheme 1a and 1b) [24]. The calcium salts were prepared from these salts by using cationic exchange resin loaded with Ca^{2+} ions as display in Fig. 3 for the parent cobaltabis(dicarbollide). After the preparation, compounds $Ca[5,6\text{-}I_2\text{-}7,8\text{-}nido\text{-}C_2B_9H_{10}]_2{\cdot}nH_2O$, $Ca[1,5,6,10\text{-}I_4\text{-}7,8\text{-}nido\text{-}C_2B_9H_8]_2{\cdot}nH_2O$, $Ca[3,3'\text{-}Co(9,12\text{-}I_2\text{-}1,2\text{-}C_2B_9H_9)_2]_2{\cdot}nH_2O$ and $Ca[3,3'\text{-}Co(8,9,10,12\text{-}I_4\text{-}1,2\text{-}C_2B_9H_7)_2]_2{\cdot}nH_2O$ were characterized by EA, ATR, MALDI-TOF-MS, ^{1}H- and ^{11}B-NMR and also Scanning Electron Microscopy (SEM). Further, thermal techniques as TGA and DSC were run to get information about the number of coordinated water molecules to the calcium. The MALDI-TOF-MS spectra of all salts display a unique peak at m/z corresponding to the molecular peak with a separation between isotopic peaks distribution of one unit, which unambiguously identifies the species as monoanionic fragments.

The $[NMe_4]^+$ or $[HNMe_3]^+$ cationic exchange by Ca^{2+} was confirmed by comparing their IR and NMR spectra. Fig. 4 displays the IR spectra of $[NMe_4][3,3'\text{-}Co(8,9,10,12\text{-}I_4\text{-}1,2\text{-}C_2B_9H_7)_2]$ and $Ca[3,3'\text{-}Co(8,9,10,12\text{-}I_4\text{-}1,2\text{-}C_2B_9H_7)_2]_2$. The IR absorption band of the N-C bond at 1476 cm^{-1} as well as its resonance at 3.45 ppm in the ^{1}H and $^1H\{^{11}B\}$ NMR spectra disappeared in the final $Ca[3,3'\text{-}Co(9,12\text{-}I_2\text{-}1,2\text{-}C_2B_9H_9)_2]_2$ and $Ca[3,3'\text{-}Co(8,9,10,12\text{-}I_4\text{-}1,2\text{-}C_2B_9H_7)_2]_2$ compounds. On the other hand, the IR spectra of the calcium tetra- and octa-iodinated compounds display several ν(O-H) at 3564 and 3357 cm^{-1} and δ(H-O-H) absorption bands at 1688, 1651 and 1598 cm^{-1}. These vibration bands indicate the presence of coordinated and non-coordinated water molecules in the formed Ca^{2+} salt. As no change is observed at the frequencies of $\nu(C_c\text{-}H)$ and ν(B-H) frequencies in the calcium derivative with respect to the corresponding $[NMe_4]^+$ or $[HNMe_3]^+$ salts, the suggested formulae are $Ca[3,3'\text{-}Co(9,12\text{-}I_2\text{-}1,2\text{-}C_2B_9H_9)_2]_2{\cdot}nH_2O$ and $Ca[3,3'\text{-}Co(8,9,10,12\text{-}I_4\text{-}1,2\text{-}C_2B_9H_7)_2]_2{\cdot}nH_2O$. Besides, the new resonances at 3.38 ppm and at 3.33 ppm (integrating 11.5 and 5.2 hydrogen atoms for each cluster (4 C_c-H)) that appears in the ^{1}H and $^1H\{^{11}B\}$ NMR spectra of $Ca[3,3'\text{-}Co(9,12\text{-}I_2\text{-}1,2\text{-}C_2B_9H_9)_2]_2$ and $Ca[3,3'\text{-}Co(8,9,10,12\text{-}I_4\text{-}1,2\text{-}C_2B_9H_7)_2]_2$, respectively, are consistent with the existence of 10 and 5 molecules of H_2O, respectively. As the Ca^{2+} cation contain coordinated H_2O molecules, the TGA/DSC studies were run to interpret whether these solvating molecules were really the easiest ones to remove. For $Ca[3,3'\text{-}Co(9,12\text{-}I_2\text{-}1,2\text{-}C_2B_9H_9)_2]_2$, an exothermic weight loss of 9.23% from room temperature to 375°C corresponds to 10 coordinated water molecules whose residual mass at 698°C is 89.68%. This value agrees with the one fount by ^{1}H-NMR spectrum.

For $Ca[3,3'\text{-}Co(8,9,10,12\text{-}I_4\text{-}1,2\text{-}C_2B_9H_7)_2]_2{\cdot}nH_2O$, the TGA/DSC displays a weight loss of 3,16%, slightly exothermic, until 240°C; which corresponds to about 5 water molecules (coordinated and possibly uncoordinated) (Fig. 5). Then a weight loss of 27.91% at 420°C in the case of $Ca[3,3'\text{-}Co(8,9,10,12\text{-}I_4\text{-}1,2\text{-}C_2B_9H_7)_2]_2{\cdot}5H_2O$ is detected, which is attributable to the loss of 6 iodine atoms. The compound decomposes at higher temperatures. Then, the formulae of the calcium salts of the anionic highly iodinated cobaltabis(dicarbollide) clusters is $Ca[3,3'\text{-}Co(9,12\text{-}I_2\text{-}1,2\text{-}C_2B_9H_9)_2]_2{\cdot}10H_2O$ and $Ca[3,3'\text{-}Co(8,9,10,12\text{-}I_4\text{-}1,2\text{-}C_2B_9H_7)_2]_2{\cdot}5H_2O$.

SEM and EDX techniques offer information about the morphology (texture) and chemical composition, respectively, of the tetra-iodinated and octa-iodinated salts at the nanometric scale (Fig. 6).

In Fig. 6a, EDX reveals the presence of calcium, iodine, boron, carbon, oxygen and cobalt in the sample of the tetra-iodinated, $Ca[3,3'\text{-}Co(9,12\text{-}I_2\text{-}1,2\text{-}C_2B_9H_9)_2]_2{\cdot}10H_2O$, and octa-iodinated, $Ca[3,3'\text{-}Co(8,9,10,12\text{-}I_4\text{-}1,2\text{-}C_2B_9H_7)_2]_2{\cdot}5H_2O$, samples. Fig.s 6b and 6c display the morphology of these samples with magnification sections obtained by SEM. The ratio of Ca/I/Co corresponds well with both formulae. The quantitative analysis of the other elements is not to be determined with this technique.

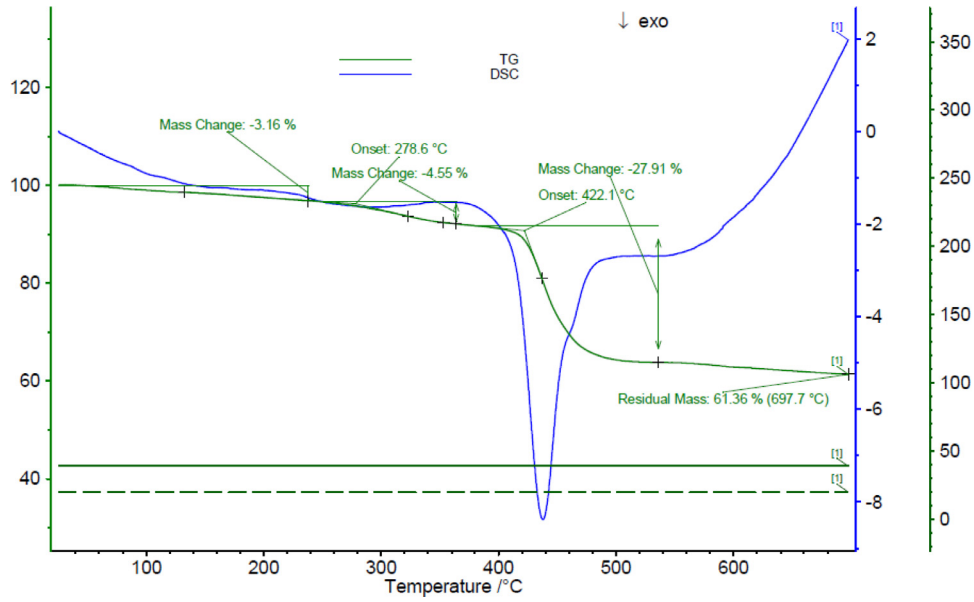

Fig. 5. TGA and DSC of Ca[3,3'-Co(8,9,10,12-I_4-1,2-$C_2B_9H_7$)$_2$]$_2$·5H_2O.

Table 1
^{1}H and ^{13}C{^{1}H} NMR chemical shifts and the IR ν(C_c-H) frequency of cobaltabis(dicarbollide) and its di-, tetra- and octa-iodinated derivatives salts. Counter cation: alkaline (Cs, Na), alkaline earth (Ca, Mg) and transition metals (Fe).

Compound	IR ν(C_c-H)	^{1}H NMR δ(C_c-H)	^{13}C NMR δ(C_c-H)
Cs[3,3'-Co(1,2-$C_2B_9H_{11}$)$_2$]	3040	3.94	51.00
Na[3,3'-Co(1,2-$C_2B_9H_{11}$)$_2$] [28]	30413031	3.97	50.99
Ca[3,3'-Co(1,2-$C_2B_9H_{11}$)$_2$]$_2$·3H_2O	3037	3.95	51.51
Mg[3,3'-Co(1,2-$C_2B_9H_{11}$)$_2$]$_2$·3H_2O	30393028	4.02	60.89
Fe[3,3'-Co(1,2-$C_2B_9H_{11}$)$_2$]$_2$	30392980	3.91	49.88
Fe[3,3'-Co(1,2-$C_2B_9H_{11}$)$_2$]$_3$	30382982	3.98	51.01
Cs[3,3'-Co(8-I-1,2-$C_2B_9H_{10}$)$_2$] [27]	3039	4.40	60.07
Na[3,3'-Co(8-I-1,2-$C_2B_9H_{10}$)$_2$] [28]	3042	3.91	50.99
Ca[3,3'-Co(8-I-1,2-$C_2B_9H_{10}$)$_2$]$_2$·3H_2O	3040	4.41	51.79
Mg[3,3'-Co(8-I-1,2-$C_2B_9H_{10}$)$_2$]$_2$·6H_2O	3040	4.41	60.83
[NMe_4][3,3'-Co(9,12-I_2-1,2-$C_2B_9H_9$)$_2$] [24]	3020	4.44	68.35
Ca[3,3'-Co(9,12-I_2-1,2-$C_2B_9H_9$)$_2$]$_2$·10H_2O	3024	4.46	49.09
[NMe_4][3,3'-Co(8,9,10,12-I_4-1,2-$C_2B_9H_7$)$_2$] [24]	3022	5.12	60.78
Ca[3,3'-Co(8,9,10,12-I_4-1,2-$C_2B_9H_7$)$_2$]$_2$·5H_2O	3024	5.13	60.78

The ^{1}H NMR and ^{13}C{^{1}H} NMR spectra (Table 1) of Ca[3,3'-Co(9,12-I_2-1,2-$C_2B_9H_9$)$_2$]$_2$·10H_2O, and Ca[3,3'-Co(8,9,10,12-I_4-1,2-$C_2B_9H_7$)$_2$]$_2$·5H_2O were run in d_6-acetone. There is practically no difference between the chemical shift of the vertex C_c-H in the two salts, [NMe_4]$^+$ and Ca^{2+}, which also supports the idea that Ca^{2+} does not interact with the anionic iodinated clusters.

3. Conclusions

Monovalent cations, Cs^+, and alkylammonium ([NR_4]$^+$) salts have traditionally been used to precipitate the anions of carboranes, boranes and metallocarboranes. In contrast, in the body and in living organisms in general, divalent cations have a special relevance. In this work, we demonstrate for the first time that these biocompatible divalent cations, of such biological importance, can also be useful to isolate the anions of borane clusters, and on the other hand, to predispose the compounds thus generated for their applications both in biology and in (bio)materials science. The preparation of Ca^{2+}, Mg^{2+} and Fe^{2+} salts of anionic iodinated *nido*-[$C_2B_9H_{12}$]$^-$ and cobaltabis(dicarbollide) as well as its di-, tetra- and octa-iodinated derivatives has been studied. Ca^{2+} and Mg^{2+} are hard Lewis acids and thus forms aqua ions if water is present in the synthetic process. All solid Ca^{2+} and Mg^{2+} salts studied in this work contained water molecules coordinated that have been detected by IR and TGA/DSC. Fe^{2+} is a medium hard Lewis acid and Fe^{3+} is a hard one. In acetone they do not coordinate to cobaltabis(dicarbollide) anion, but are solvated by acetone. The studied Ca^{2+} salts of iodinated cobaltabis(dicarbollides) are small molecules that do two tasks: incorporate the divalent Ca^{2+} cations as a bone component to act as molecular glue interacting with bone's collagen and incorporate anions with iodine atoms that would provide radiopacity. These purely inorganic small molecules are good candidates for biomedical application because offer an opportunity to be applied as X-ray contrast in regenerative medicine and/or in bone defect repair. More research on this field that will appear when finished is going on in our laboratories.

4. Materials and methods

4.1. Instrumentation

Elemental analyses were performed using a Carlo Erba EA1108 microanalyzer. ATR-IR spectra (ν, cm^{-1}) were obtained on a Shimadzu FTIR-8300 spectrophotometer. The ^{1}H and ^{1}H{^{11}B} NMR (300.13 MHz), ^{13}C{^{1}H} NMR (75.47 MHz) and ^{11}B and ^{11}B{^{1}H} NMR (96.29 MHz) spectra were recorded on a Bruker ARX 300

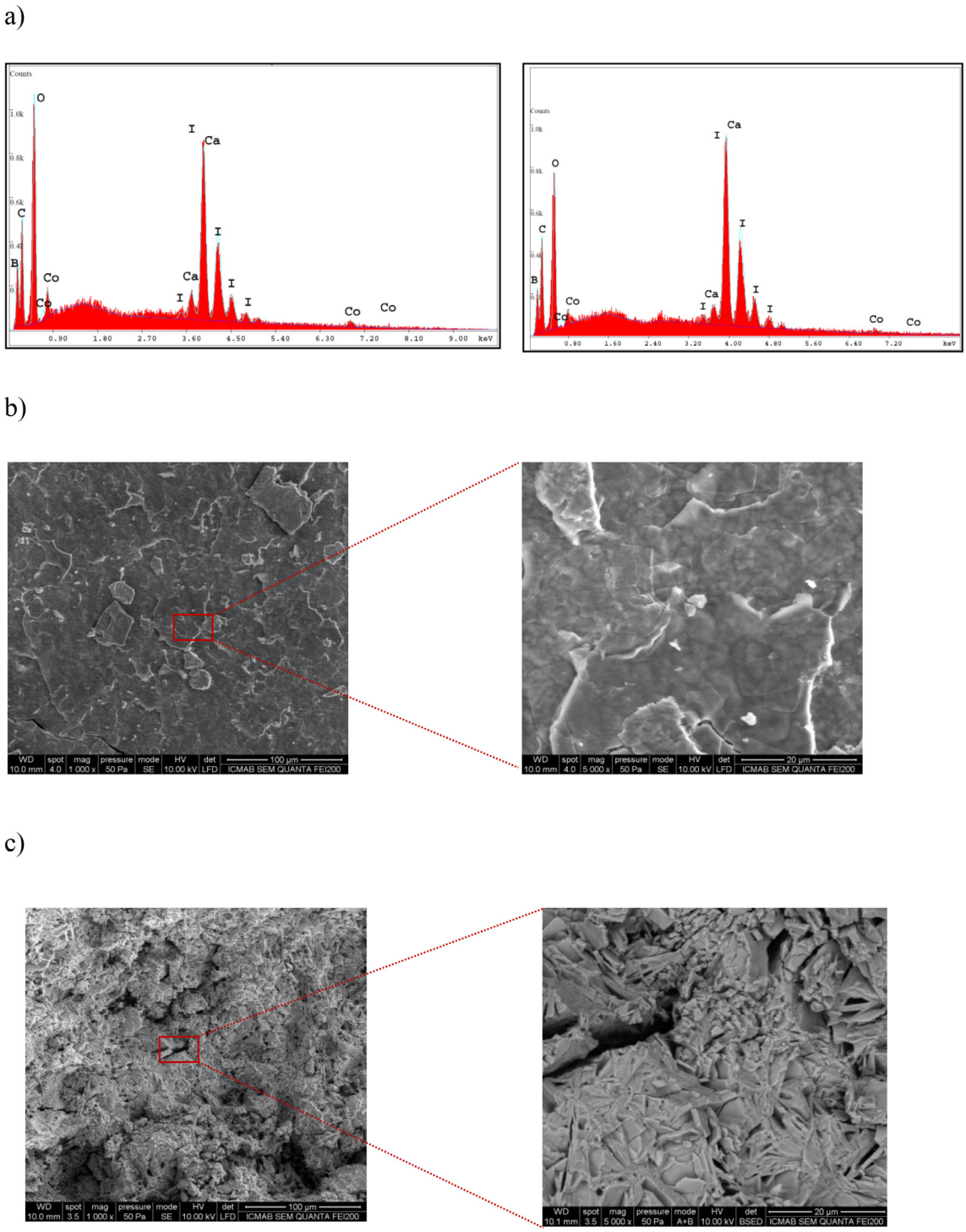

Fig. 6. a) EDX of Ca[3,3'-Co(9,12-I_2-1,2-$C_2B_9H_9$)$_2$]$_2$·10H_2O (left) and Ca[3,3'-Co(8,9,10,12-I_4-1,2-$C_2B_9H_7$)$_2$]$_2$·5H_2O. b) SEM images of Ca[3,3'-Co(9,12-I_2-1,2-$C_2B_9H_9$)$_2$]$_2$·10H_2O, scale bar 100 μm (left) and its magnification, scale bar 20 μm (right); c) SEM images of Ca[3,3'-Co(8,9,10,12-I_4-1,2-$C_2B_9H_7$)$_2$]$_2$·5H_2O, scale bar 100 μm (left) and its magnification, scale bar 20 μm (right).

instrument equipped with the appropriate decoupling accessories. Exception for the compounds Ca[3,3'-Co(1,2-$C_2B_9H_{11}$)$_2$]$_2$, Mg[3,3'-Co(1,2-$C_2B_9H_{11}$)$_2$]$_2$, Ca[3,3'-Co(8-I-1,2-$C_2B_9H_{10}$)$_2$]$_2$ and Mg[3,3'-Co(8-I-1,2-$C_2B_9H_{10}$)$_2$]$_2$ that were run on a Bruker Avance-III 400MHz (9.4 T) instrument also equipped with the appropriate decoupling accessories. All NMR spectra were performed in acetone deuterated solvent at 22°C. The ^{11}B and ^{11}B{^{1}H} NMR shifts were referenced to external BF_3·OEt_2, while the ^{1}H, ^{1}H{^{11}B} and ^{13}C{^{1}H} NMR shifts were referenced to $SiMe_4$. Chemical shifts are reported in units of parts per million downfield from the reference, and all coupling constants are reported in Hertz. The mass spectra were recorded in the negative ion mode using a Bruker Biflex MALDI-TOF-MS (N_2 laser; λ_{exc} 337 nm (0.5 ns pulses); voltage ion source 20.00 kV (Uis1) and 17.50 kV (Uis2)). Thermogravimetric Analyses (TGA) and Differential Scanning Calorimetry (DSC) were performed on a Netzsch STA 449 thermal analyzer at a heating rate of 10°C/min in an Ar atmosphere. Transmission electron microscopy (TEM) studies were carried out using JEOL JEM 1210 at

120 kV. Scanning Electron Microscope (SEM) were performed using Quanta FEI 200 FEG-ESEM operating at an acceleration voltage of 15 kV and low vacuum. The microscope is equipped with an Oxford Inca Energy Dispersive X-ray (EDAX) system for chemical analysis in which qualitative and quantitative analysis can be performed by the software Genesis Spectrum version 5.21.

4.2. Materials

Experiments were carried out, except when noted, under a dry, oxygen-free dinitrogen atmosphere using standard Schlenk techniques, with some subsequent manipulation in the open laboratory. I_2, K_2CO_3 and Na_2SO_3 were purchased from Sigma-Aldrich. Acetone was reagent grade and was obtained by distillation from appropriate drying agent before using. Dichloromethane, diethyl ether, acetonitrile were purchased from Carlo Erba Reagents. Silica gel for preparative layer chromatography (containing a 13% of calcium sulphate) was purchased from Fluka Analytical. [$HNMe_3$][5,6-I_2-7,8-*nido*-$C_2B_9H_{10}$], [24,25] [$HNMe_3$][1,5,6,10-I_4-7,8-*nido*-$C_2B_9H_8$], [24,25] Cs[3,3'-Co(1,2-$C_2B_9H_{11}$)$_2$], [26] Ag[3,3'-Co(1,2-$C_2B_9H_{11}$)$_2$], [21] Cs[3,3'-Co(8-I-1,2-$C_2B_9H_{10}$)$_2$], [27] [NMe_4][3,3'-Co(9,12-I_2-1,2-$C_2B_9H_9$)$_2$], [24] and [NMe_4][3,3'-Co(8,9,10,12-I_4-1,2-$C_2B_9H_7$)$_2$], [24] were prepared according to the literature.

4.3. I. Synthetic procedure of iron salts

4.3.1. Synthesis and characterization of Fe[3,3'-Co(1,2-$C_2B_9H_{11}$)$_2$]$_2$

Under a nitrogen atmosphere, $FeCl_2$ (44.4 mg, 0.35 mmol) was added to a 50 ml of deoxygenated ethanol. solution of Ag[3,3'-Co(1,2-$C_2B_9H_{11}$)$_2$] (300 mg, 0.7 mmol). The white precipitate (AgCl) was removed by filtration and weighed (~2 equiv), and the resulting orange/brownish solution was evaporated. A pure orange stable solid of Fe[3,3'-Co(1,2-$C_2B_9H_{11}$)$_2$]$_2$ was obtained. Yield: 243.7 mg, 99%. IR (ATR): ν(cm^{-1})= 3529 (vs, ν(O-H)), 3039, 2980 (s, ν($C_{cluster}$-H)), 2564, 2517 (vs, ν(B-H)), 1607 (s, δ(H-O-H)). ^{1}H NMR (CD_3COCD_3): δ= 3.91 (br s, 4H, $C_{cluster}$-*H*), 3.50-1.40 (br s, 18H, B-*H*); ^{1}H{^{11}B} NMR (CD_3COCD_3): δ= 3.91 (br s, 4H, $C_{cluster}$-*H*), 3.28 (br s, 2H, B-*H*), 2.92 (br s, 2H, B-*H*), 2.64 (br s, 4H, B-*H*), 1.81 (br s, 4H, B-*H*), 1.60 (br s, 2H, B-*H*), 1.52 (br s, 4H, B-*H*); ^{13}C{^{1}H} NMR (CD_3COCD_3): δ= 49.88 ($C_{cluster}$). ^{11}B NMR (CD_3COCD_3): δ= 7.6 (d, ^1J(B,H) = 141 Hz, 2B), 2.5 (d, ^1J(B,H) = 140 Hz, 2B), -4.9 (8B), -16.2 (d, ^1J(B,H) =154 Hz, 4B), -21.7 (d, ^1J(B,H) =166 Hz, 2B). MALDI-TOF-MS (m/z) calcd for [Co($C_2B_9H_{11}$)$_2$]$^-$: 324.76; found:324.35 (M, 100%,) where M is the molecular weight of the anion [3,3'-Co(1,2-$C_2B_9H_{11}$)$_2$]$^-$.

4.3.2. Synthesis and characterization of Fe[3,3'-Co(1,2-$C_2B_9H_{11}$)$_2$]$_3$

Under inert nitrogen atmosphere, $FeCl_3$ (37.9 mg, 0.23 mmol) was added to a 50 ml of deoxygenated ethanol solution of Ag[3,3'-Co(1,2-$C_2B_9H_{11}$)$_2$] (300 mg, 0.7 mmol). The white AgCl precipitate was removed by filtration and weighed (~3 equiv), and the resulting orange/brownish solution was evaporated. A pure stable to air solid of Fe[3,3'-Co(1,2-$C_2B_9H_{11}$)$_2$]$_3$ was obtained. Yield: 237.3 g, 99%. IR (ATR): ν(cm^{-1})= 3508 (s, ν(O-H)), 3038, 2982 (s, ν($C_{cluster}$-H)), 2933, 2908 (w, ν($C_{cluster}$-H)), 2563, 2525 (vs, ν(B-H)) and 1609 (w, δ(H-O-H). ^{1}H NMR (CD_3COCD_3): δ= 3.98 (br s, 4H, $C_{cluster}$-*H*), 3.44 (q, ^1J(H,H)= 6 Hz, CH_3-CH_2OH), 3.60-1.30 (br s, 18H, B-*H*), 1.11 (t, ^1J(H,H)= 6 Hz, CH_3-CH_2OH). ^{1}H{^{11}B} NMR (CD_3COCD_3): δ= 3.98 (br s, 4H, $C_{cluster}$-*H*), 3.44 (br s, CH_3-CH_2OH), 3.02, 2.75, 1.98, 1.66, 1.60, 1.39 (br s, 18H, B-*H*). ^{13}C{^{1}H} NMR (CD_3COCD_3): δ= 153.69 (s, CH_3-CH_2OH), 51.01 ($C_{cluster}$). ^{11}B NMR (CD_3COCD_3): δ= 8.2 (d, ^1J(B,H) = 142 Hz, 2B), 3.0 (d, ^1J(B,H) = 139 Hz, 2B), -4.3 (d, ^1J(B,H) = 141 Hz, 8B), -15.6 (d, ^1J(B,H) =153 Hz, 4B), -21.1 (d, ^1J(B,H) =167 Hz, 2B). MALDI-TOF-MS (m/z) calcd for [Co($C_2B_9H_{11}$)$_2$]$^-$: 324.76; found:323.84 (M, 100%,) where M is the molecular weight of the anion [3,3'-Co(1,2-$C_2B_9H_{11}$)$_2$]$^-$.

4.4. II. Synthetic procedure of calcium and magnesium salts

4.4.1. General procedure of cationic exchange resin

To get the calcium salts species, the starting compounds [$HNMe_3$][5,6-I_2-7,8-*nido*-$C_2B_9H_{10}$]$_2$, [$HNMe_3$][1,5,6,10-I_4-7,8-*nido*-$C_2B_9H_8$]$_2$, [NMe_4][3,3'-Co(9,12-I_2-1,2-$C_2B_9H_9$)$_2$], [NMe_4][3,3'-Co(8,9,10,12-I_4-1,2-$C_2B_9H_7$)$_2$], [NMe_4][3,3'-Co(1,2-$C_2B_9H_{11}$)$_2$] and Cs[3,3'-Co(8-I-1,2-$C_2B_9H_{10}$)$_2$] were dissolved in a minimum volume of acetonitrile/water (50/50). Then, each solution was passed repeatedly through a cation exchange resin, previously loaded with calcium. The solvent was finally evaporated. The disappearance of the [NMe_4]$^+$ and [$HNMe_3$]$^+$ peaks in the IR and ^{1}H NMR spectra was a clear indication that the complete exchange to calcium was successful.

4.4.2. Characterization of Ca[5,6-I_2-7,8-nido-$C_2B_9H_{10}$]·5H_2O

IR (ATR): ν(cm^{-1})= 2536 (vs, ν(B-H)), 1696 (s, δ(H-O-H)), 1656 (s, δ(H-O-H)), 1608 (vs, δ(H-O-H)). ^{1}H NMR (CD_3COCD_3): δ= 4.19 (br s, 2H, $C_{cluster}$-*H*). ^{1}H{^{11}B} NMR (CD_3COCD_3): δ= 4.17 (s, H_2O), 2.46, 1.86, 1.78, 1.14 (s, 7H, B-*H*), 1.08 (d, ^1J (H_{bridge}-H)= 9Hz, 1H, BH), -2.13 (d, ^1J (H_{bridge}-H)= 9Hz, 1H, B-H_{bridge}). ^{11}B NMR (CD_3COCD_3): δ= -8.6 (d, 2B, ^1J(B,H) = 141 Hz, 2B, B(9,11)), -16.2 (d, ^1J(B,H) = 162 Hz, 1B, B(3)), -20.3 (d, ^1J(B,H) = 155 Hz, 2B, B(2,4), -23.3 (br s, 2B, B(5,6)), -27.0 (dd, ^1J(B,H) = 134 Hz, ^1J(H,H) = 9 Hz 1B, B(10)), -32.8 (d, ^1J(B,H) = 148 Hz, 1B, B(1)). MALDI-TOF-MS (m/z): 387.05 (M, 100%,) where M is the molecular weight of the anion [5,6-I_2-7,8-*nido*-$C_2B_9H_{10}$]$^-$. TGA/DSC: a light exothermic weight loss of 10.30% until 172°C and a continued exothermic weight loss to residual mass of 75.96% observed until 678°C.

4.4.3. Characterization of Ca[1,5,6,10-I_4-7,8-nido-$C_2B_9H_8$]$_2$·4H_2O

IR (ATR): ν(cm^{-1})= 3544, 3483 (s, ν(O-H)), 3011, 2909 (s, ν($C_{cluster}$-H)), 2569 (vs, ν(B-H)), 1688 (vs, δ(H-O-H)), 1655 (s, δ(H-O-H)), 1609 (s, δ(H-O-H)). ^{1}H NMR (CD_3COCD_3): δ= 4.06 (br s, H_2O), 2.54 (br s, 2H, $C_{cluster}$ -*H*). ^{1}H{^{11}B} NMR (CD_3COCD_3): δ= 4.06 (br s, H_2O), 2.67 (br s, B-*H*), 2.55 (br s, 2H, $C_{cluster}$-*H*), 2.21 (s, B-*H*), -0.04 (br s, 1H, B-H_{bridge}). ^{11}B NMR (CD_3COCD_3): δ= -8.6 (d, ^1J(B,H) = 147 Hz, 2B, B(9,11)-*H*), -16.1 (d, 1B, B(3)*H*), -17.9 (4B, B(5,6)-*I* + B(2,4)-*H*), -35.4 (s, 2B, B(1,10)-*I*). MALDI-TOF-MS (m/z): 636.7 (M, 100%,) where M is the molecular weight of the anion [1,5,6,10-I_4-7,8-*nido*-$C_2B_9H_8$]$^-$. TGA/DSC: a light exothermic weight loss of 5.39% until 200°C and a continued exothermic weight loss to residual mass of 67.60% observed until 698°C.

4.4.4. Characterization of Ca[3,3'-Co(1,2-$C_2B_9H_{11}$)$_2$]$_2$·3H_2O

IR (ATR): ν(cm^{-1})= 3540 (s, ν(,O-H)), 3037 (s, ν($C_{cluster}$-H)), 2532 (vs, ν(B-H)) 1603 (vs, δ(H-O-H)). ^{1}H NMR (CD_3COCD_3): δ=3.95 (s, 4H, $C_{cluster}$ -*H*); 3.16 (s, H_2O). ^{1}H{^{11}B} NMR (CD_3COCD_3): δ=3.95 (s, 4H, $C_{cluster}$-*H*), 3.40 (s, 2H, B-*H*), 3.15 (s, H_2O), 2.98 (s, 2H, B-*H*), 2.72 (s, 4H, B-*H*), 1.94 (s, 4H, B-*H*), 1.63 (s, 2H, B-*H*), 1.57 (s, 2H, B-*H*). ^{11}B NMR (CD_3COCD_3): δ= 6.4 (d, ^1J(B,H) = 147 Hz, 2B, B(8)-*H*), 1.2 (d, ^1J(B,H) = 142 Hz, 2B, B(10)-*H*), -5.5 (d, 4B, B(4,7)-*H*), -6.2 (d, 4B, B(9,11)-*H*), -17.5 (d, ^1J(B,H) = 156 Hz, 2B, B(5,11)-*H*), -23.0 (d, ^1J(B,H) = 169 Hz, 4B, B(6)-*H*). MALDI-TOF-MS (m/z) calcd for [Co($C_2B_9H_{11}$)$_2$]$^-$: 324.76; found: 324.04 (M, 100%,) where M is the molecular weight of the anion [3,3'-Co(1,2-$C_2B_9H_{11}$)$_2$]$^-$. TGA/DSC: a weight loss of 7.05% until 120°C followed by a weight loss of 3.50% at 175°C were observed. Anal. Calcd. for $C_8H_{50}B_{36}CaCo_2O_3$: 12.95, H: 6.79. Found: C: 12.81, H: 6.92.

4.4.5. Characterization of Ca[3,3'-Co(8-I-1,2-$C_2B_9H_{10}$)$_2$]$_2$·3H_2O

IR (ATR): ν(cm^{-1})= 3562 (w, ν(O-H)), 3040 (s, ν($C_{cluster}$-H)), 2612, 2584, 2533 (vs, ν(B-H)) 1604, (δ(H-O-H)). ^{1}H NMR (CD_3COCD_3): δ=4.41 (s, 4H, $C_{cluster}$ -*H*), 3.00 (s, H_2O). ^{1}H{^{11}B} NMR (CD_3COCD_3): δ=4.41 (s, 4H, $C_{cluster}$-*H*), 3.24 (s, 4H, B-*H*), 3.22 (s, 2H, B-*H*), 3.07 (s, 2H, B-*H*), 3.00 (s, H_2O), 2.60 (s, 4H, B-*H*), 2.12

(s, 2H, B-*H*), 1.84 (s, 4H, B-*H*). ^{11}B NMR (CD_3COCD_3): δ= 2.8 (d, ^1J(B,H) = 147 Hz, 2B, B(10)-*H*), -3.4 (d, 8B, B(4,7,9,11)-*H*), -5.3 (d, 2B, B(8)-*I*), -17.1 (d, ^1J(B,H) = 159 Hz, 4B, B(5,11)-*H*), -22.6 (d, ^1J(B,H) = 173 Hz, 2B, B(6)-*H*). MALDI-TOF-MS (m/z): 575.66 (M, 100%,) where M is the molecular weight of the anion [3,3'-Co(8-I-1,2-$C_2B_9H_{10})_2]^-$. TGA/DSC: two exothermic weight loss of 4.17% and 8.98% in the ranges 80-120°C and 120-180°C, respectively, were observed. Anal. Calcd. for $C_8H_{46}B_{36}CaCo_2I_4O_3$: C: 7.72, H: 3.72. Found: C: 7.53, H: 3.83.

4.4.6. Characterization of Ca[3,3'-Co(9,12-I_2-1,2-$C_2B_9H_9)_2]_2$·10H_2O

IR (ATR): ν(cm^{-1})= 3024 (s, ν($C_{cluster}$-H)), 2580 (vs, ν(B-H)), 1696(w, δ(H-O-H)), 1660(s, δ(H-O-H)), 1608 (vs, δ(H-O-H)). ^{1}H NMR (CD_3COCD_3): δ= 4.46 (br s, 4H, $C_{cluster}$-*H*), 3.38 (br s, H_2O). ^{1}H{^{11}B} NMR (CD_3COCD_3): δ= 4.46 (br s, 4H, $C_{cluster}$-*H*), 4.22, 3.65 (br s, H,B-*H*), 3.38 (br s, H_2O), 1.66 (br s, B-*H*). ^{13}C{^{1}H} NMR (CD_3COCD_3): δ= 49.09 ($C_{cluster}$). ^{11}B NMR (CD_3COCD_3): δ= 8.3 (d, ^1J(B,H) = 157 Hz, 2B, B(8,8')), 5.9 (d, ^1J(B,H) = 173 Hz, 2B, B(10,10')), -4.3 (d, ^1J(B,H) = 153 Hz, 4B, B(4,4',7,7'), -14.1 (d, ^1J(B,H) = 131 Hz, 4B, B(5,5',11,11'), -14.0 (s, 4B, B(9,9',12,12')), -20.9 (d, ^1J(B,H) = 162 Hz, 2B, B(6,6')). MALDI-TOF-MS (m/z): 827.8 (M, 100%,) where M is the molecular weight of the anion [3,3'-Co(9,12-I_2-1,2-$C_2B_9H_9)_2]^-$. TGA/DSC: a light exothermic weight loss of 9.23% until 375°C, the residual mass is 89.68% at 698°C. Anal. Calcd. for $C_8H_{46}B_{36}CaCo_2I_8O_{10}$: C: 5.15, H: 2.49. Found: C: 5.31, H: 2.60.

4.4.7. Characterization of Ca[3,3'-Co(8,9,10,12-I_4-1,2-$C_2B_9H_7)_2]_2$·5H_2O

IR (ATR): ν(cm^{-1})= 3564, 3357 (w, ν(O-H)), 3024 (s, ν($C_{cluster}$-H)), 2620, 2583 (vs, ν(B-H)), 1688 (s, δ(O-H)), 1652 (s, δ(O-H)), 1599 (s, δ(O- H)). ^{1}H NMR (CD_3COCD_3): δ= 5.13 (br s, 4H, $C_{cluster}$-*H*), 3.33 (br s, H_2O); ^{1}H{^{11}B} NMR (CD_3COCD_3): δ= 5.14 (br s, 4H, $C_{cluster}$-H), 3.63, 2.78 and 2.68 (br s, B-*H*); ^{13}C{^{1}H} NMR (CD_3COCD_3): δ= 60.78 ($C_{cluster}$); ^{11}B NMR (CD_3COCD_3): δ= -1.7 (d, ^1J(B,H) =154 Hz, 4B, B(4,4',7,7'), -3.7 (s, 2B, B(8,8')), -6.7 (s, 2B, B(10,10')), -9.7 (s, 4B, B(9,9',12,12')), -13.1 (d, ^1J(B,H) =151 Hz, 4B, B(5,5',11,11')), -20.2 (d, ^1J(B,H) = 167 Hz, 2B, B(6,6')). MALDI-TOF-MS (m/z): 1331.1 (M, 100%,) where M is the molecular weight of the anion [3,3'-Co(8,9,10,12-I_4-1,2-*closo*-$C_2B_9H_7)_2]^-$. TGA/DSC: a light exothermic weight loss of 3,16% until 240°C and an exothermic weight loss of 27.91% at 420°C arriving to a residual mass 61.36% at 698°C. Anal. Calcd. for $C_8H_{38}B_{36}CaCo_2I_{16}O_5$: C: 3.44, H: 1.37. Found: C: 3.77, H: 1.41.

4.4.8. Characterization of Mg[3,3'-Co(1,2-$C_2B_9H_{11})_2]_2$·3H_2O

IR (ATR): ν(cm^{-1})= 3580, 3516 (s, ν(,O-H)), 3039, 3028 (s, ν($C_{cluster}$-H)), 2581, 2512 (vs, ν(B-H)), 1644, 1600 (δ(H-O-H)). ^{1}H NMR (CD_3COCD_3): δ=4.02 (br s, H_2O), 3.95 (s, 4H, $C_{cluster}$ -*H*). ^{1}H{^{11}B} NMR (CD_3COCD_3): δ=4.02 (br s, H_2O), 3.95 (s, 4H, $C_{cluster}$ -*H*); 3.40 (s, 2H, B-*H*), 2.98 (s, 2H, B-*H*), 2.71 (s, 4H, B-*H*), 1.94 (s, 4H, B-*H*), 1.63 (s, 2H, B-*H*), 1.57 (s, 4H, B-*H*). ^{11}B NMR (CD_3COCD_3): δ= 6.3 (d, ^1J(B,H) = 142 Hz, 2B, B(8)-*H*), 1.2 (d, ^1J(B,H) = 147 Hz, 2B, B(10)-*H*), -5.6 (d, 4B, B(4,7)-*H*), -6.3 (d, 4B, B(9,11)-*H*), -17.5 (d, ^1J(B,H) = 154 Hz, 2B, B(5,11)-*H*), -23.0 (d, ^1J(B,H) = 165 Hz, 4B, B(6)-*H*). MALDI-TOF-MS (m/z) calcd for $[Co(C_2B_9H_{11})_2]^-$: 324.76; found: 324.03 (M, 100%,) where M is the molecular weight of the anion [3,3'-Co(1,2-$C_2B_9H_{11})_2]^-$. TGA/DSC: two exothermic weight loss of 3,10 and 4.33% in the temperature range 9-200°C.. Anal. Calcd. for $C_8H_{50}B_{36}Co_2MgO_3$: C: 13.24, H: 6.94. Found: C: 13.64, H: 7.15.

4.4.9. Characterization of Mg[3,3'-Co(8-I-1,2-$C_2B_9H_{10})_2]_2$·6H_2O

IR (ATR): ν(cm^{-1})= 3584 (w, ν(O–H)), 3040 (s, ν($C_{cluster}$-H)), 2610, 2579, 2532 (vs, ν(B-H)), 1602 (δ(H-O-H)). ^{1}H NMR (CD_3COCD_3): δ=4.40 (s, 4H, $C_{cluster}$ -*H*), 4.15 (br s, H_2O). ^{1}H{^{11}B} NMR (CD_3COCD_3): δ=4.41 (s, 4H, $C_{cluster}$-*H*), 4.14 (br s, H_2O), 3.23 (s, 5H, B-*H*), 3.06 (s, 2H, B-*H*), 2.59 (s, 5H, B-*H*), 2.12 (s, 2H, B-*H*), 1.83 (s, 4H, B-*H*). ^{11}B NMR (CD_3COCD_3): δ= 2.8 (d, ^1J(B,H) = 147 Hz, 2B, B(10)-*H*), -3.4 (d, 8B, B(4,7,9,11)-*H*), -5.4 (d, 2B, B(8)-*I*), -17.1 (d, ^1J(B,H) = 160 Hz, 4B, B(5,11)-*H*), -22.7 (d, ^1J(B,H) = 172 Hz, 2B, B(6)-*H*). MALDI-TOF-MS (m/z): 575.66 (M, 100%,) where M is the molecular weight of the anion [3,3'-Co(8-I-1,2-$C_2B_9H_{10})_2]^-$. TGA/DSC: two exothermic weight loss of 4,86 and 3.44% since 200°C. Anal. Calcd. for $C_8H_{52}B_{36}Co_2MgI_4O_6$: C: 7.49, H: 4.08. Found: C: 7.19, H: 4.22.

Declaration of Competing Interest

The authors declare that they have no known competing financial interests or personal relationships that could have appeared to influence the work reported in this paper.

Acknowledgements

This work has been supported by the Spanish Ministerio de Economía y Competitividad (CTQ2016-75150-R) and the Generalitat de Catalunya (2017SGR1720). Miquel Nuez is enrolled in the PhD program of the UAB.

Supplementary materials

Supplementary material associated with this article can be found, in the online version, at doi:10.1016/j.jorganchem.2021.121997.

References

[1] a) G. Kass, S. Orrenius, Environ Health Perspect 107 (1999) 25–35; b) R. Roskoski, Pharmacol. Res. 100 (2015) 1–23; c) M.A. Ditzler, M. Otyepka, J. Sponer, N. G.Walter, Acc. Chem. Res. 43 (1) (2010) 40–47.
[2] P. Chellan, P.J. Sadler, Phil. Trans. R. Soc. A 373 (2015) 20140182.
[3] a) D. Crowfoot Hodgkin, J. Kamper, M. Mackay, J. Pickworth, K.N. Trueblood, J.G. White, 1956 Nature, 178 64–66; b) D. Crowfoot, Hodgkin was awarded with the 1964 Nobel Prize in Chemistry for her determinations by X-ray techniques of the structures of important biochemical substances, 1964.
[4] a) N. Reznikov, M. Bilton, L. Lari, M.M. Stevens, R. Kröger, Science 360 (6388) (2018) eaao2189; b) K. Grandfield, V. Vuong, H.P. Schwarcz, Calcif. Tissue Int. 103 (2018) 606–616.
[5] M.J. Glimcher, Rev. Mineral. Geochem. 64 (2006) 223–282.
[6] a) K. Leach, F.M. Hannan, T.M. Josephs, A.N. Keller, T.C. Moller, D.T. Ward, E. Kallay, R.S. Mason, R.V. Thakker, D. Riccardi, A.D. Conigrave, H. Brauner-Osborne, Pharmacol. Rev. 72 (3) (2020) 558–604; b) W.R. Gombotz, S.F. Wee, Adv. Drug Deliv. Rev. 64 (2012) 194–205.
[7] B. Jay, S.H. Ahn, Semin. Interv. Radiol. 30 (3) (2013) 297–306.
[8] a) N. Patel, Phys Med Rehabil Clin N Am 21 (2010) 869–876; b) C.T. McConnell Jr., F.J. Wippold, C.E. Ray, B.N. Weissman, P.D. Angevine, I.B. Fries, L.T. Holly, B.S. Kapoor, J.M. Lorenz, J.S. Luchs, J.E. O'Toole, N.D. Patel, C.J. Roth, D.A. Rubin, J Am Coll Radiol 11 (8) (2014) 757–763.
[9] a) G. Lewis, L.H. Koole, C.S. van Hooy-Corstjens, J Biomed Mater Res B Appl Biomater 91 (2009) 537–544; b) E.J. Boelen, G. Lewis, J. Xu, T. Slots, L.H. Koole, C.S. van Hooy-Corstjens, J Biomed Mater Res A 86 (1) (2008) 76–88; c) G. Lewis, J. Biomed. Mater. Res. Part B Appl. Biomater 81 (2) (2007) 371–386.
[10] S.B. Yu, A.D. Watson, Chem. Rev. 99 (1999) 2353–2378.
[11] a) J. Poater, M. Solà, C. Viñas, F. Teixidor, Angew. Chemie - Int. Ed. 53 (2014) 12191–12195; b) J. Poater, C. Viñas, I. Bennour, S.E. Gordils, M. Solà, F. Teixidor, J. Am. Chem. Soc. 142 (20) (2020) 9396–9407.
[12] a) Handbook of boron science: with applications in organometallics, catalysis, materials and medicine, 2019. Vol 4: Boron in Medicine. Eds. Hosmane, NS; Eagling, R. World Scientific Europe Ltd; b) E. Hey-Hawkins, C. Viñas (Eds.), Boron-Based Compounds. Potential and Emerging applications in Medicine, John Wiley & Sons Ltd, Chichester, UK, 2018; c) P. Stockmann, M. Gozzi, R. Kuhnert, M.B. Sarosi, E. Hey-Hawkins, 2019 Chem. Soc. Rev., 48 3497–3512; d) F. Issa, M. Kassiou, L. Rendina, 2011 Chem. Rev., 111 5701–5722; e) E.Hey-Hawkins M.Scholz, 2011 Chem. Rev., 111 7035–7062; f) Z. Lesnikowski, 2019 J. Med. Chem., 59 7738–7758; g) J. Plesek, 1992 Chem. Rev., 92 269–278.
[13] C. Viñas, Future Med. Chem. 5 (6) (2013) 617–619.
[14] A. Pepiol, F. Teixidor, K. Saralidze, C. van der Marel, P. Willems, L. Voss, M.L.W. Knetsch, C. Viñas, L.H. Koole, Biomaterials 32 (2011) 6389–6398.
[15] a) R.A. Wiesboeck, M.F. Hawthorne, J. Am. Chem. Soc. 86 (1964) 1642–1643 By alkoxides; b) M.F. Hawthorne, D.C. Young, P.M. Garret, D.A. Owen, S.G. Schwerin, F.N. Tebbe, P.M. Wegner, J. Am. Chem. Soc. 90 (4) (1968) 862–868.
[16] a) L.I. Zakharkin, V.N. Kalinin, Tetrahedron Lett 6 (7) (1965) 407–409 By amines; b) Y. Taoda, T. Sawabe, Y. Endo, K. Yamaguchi, S. Fujii, H. Kagechika, Chem. Commun. (2008) 2049–2051.

[17] By fluorides: M.A. Fox, W.R. Gill, P.L. Herbertson, J.A.H. MacBride, K. Wade, Polyhedron 16 (1996) 565–571.
[18] By phosphanes: M.G. Davidson, M.A. Fox, T.G. Hibbert, J.A.K. Howard, A. Mackinnon, I.S. Neretin, K. Wade, Chem. Commun. (1999) 1649–1650.
[19] a) I.B. Sivaev, V.I. Bregadze, Collect. Czech. Chem. Commun. 64 (5) (1999) 783–805; b) I.B. Sivaev, V.I. Bregadze, Collect. Czech. Chem. Commun. 614 (2002) 27–36; c) M.F. Hawthorne, J.I. Zink, J.M. Skelton, M.J. Bayer, C. Liu, E. Livshits, R. Baer, D. Neuhauser, Science 303 (2004) 1849–1851; d) R.D. Kennedy, C.B. Knobler, M.F. Hawthorne, Inorg. Chem. 48 (19) (2009) 9377–9384.
[20] A. Zaulet, F. Teixidor, P. Bauduin, O. Diat, P. Hirva, A. Ofori, C. Viñas, J. Organomet. Chem. 865 (2018) 214–225.
[21] Z. Xie, T. Jelinek, R. Bau, C.A. Reed, J. Am. Chem. Soc. 116 (1994) 1907–1913.
[22] a) M.F. Hawthorne, T.D. Andrews, J. Chem. Soc., Chem. Commun. (1965) 443–444; b) M.F. Hawthorne, D.C. Young, P.A. Wegner, J. Am. Chem. Soc. 87 (1965) 1818–1819; c) A.M. Cioran, F. Teixidor, C. Viñas, Dalton Trans 44 (2015) 2809–2818; d) T.O. Pennanen, J. Machácek, S. Taubert, J. Vaara, D. Hnyk, Phys. Chem. Chem. Phys. 12 (2010) 7018–7025.
[23] H.M.N.H. Irving, R.J.P. Williams, J. Chem. Soc. (1953) 3192–3210.
[24] A. Pepiol, F. Teixidor, R. Sillanpää, M. Lupu, C. Viñas, Angew. Chem. Int. Ed. 50 (2011) 12491–12495.
[25] F. Teixidor, C. Viñas, Halogenated Icosahedral Carboranes: A Platform for Remarkable Applications, Handbook of boron science: with applications in organometallics, catalysis, materials and medicine 1 (2019) 205–228 Boron in organometallic chemistry. Eds. Hosmane, NS; Eagling, R.
[26] M.F. Hawthorne, D.C. Young, T.D. Andrews, D.V. Howe, R.L. Pilling, A.D. Pitts, M. Reintjes, L.F. Warren, P.A. Wegner, J. Am. Chem. Soc. 90 (1968) 879–896.
[27] I. Rojo, F. Teixidor, R. Kivekäs, R. Sillanpää, C. Viñas, Organometallics 22 (2003) 4642–4646.
[28] I. Fuentes, A. Andrio, F. Teixidor, C. Viñas, V. Compan, Phys. Chem. Chem. Phys. 19 (2017) 15177–15186.